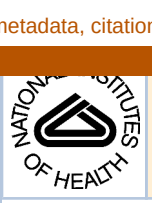

Published in final edited form as:

J Biol Chem. 2008 March 7; 283(10): 6321–6329. doi:10.1074/jbc.M707353200.

Single Channel Properties of Heterotetrameric Mutant RyR1 Ion Channels Linked to Core Myopathies[*,S]

Le Xu, **Ying Wang**, **Naohiro Yamaguchi**, **Daniel A. Pasek**, and **Gerhard Meissner**[1]

From the Department of Biochemistry and Biophysics, University of North Carolina, Chapel Hill, North Carolina 27599-7260

Abstract

Skeletal muscle excitation-contraction coupling involves activation of homotetrameric ryanodine receptor ion channels (RyR1s), resulting in the rapid release of Ca^{2+} from the sarcoplasmic reticulum. Previous work has shown that Ca^{2+} release is impaired by mutations in RyR1 linked to Central Core Disease and Multiple Minicore Disease. We studied the consequences of these mutations on RyR1 function, following their expression in human embryonic kidney 293 cells and incorporation in lipid bilayers. RyR1-G4898E, -G4898R, and -ΔV4926/I4927 mutants in the C-terminal pore region of RyR1 and N-terminal RyR1-R110W/L486V mutant all showed negligible Ca^{2+} permeation and loss of Ca^{2+}-dependent channel activity but maintained reduced K^+ conductances. Co-expression of wild type and mutant RyR1s resulted in Ca^{2+}-dependent channel activities that exhibited intermediate Ca^{2+} selectivities compared with K^+, which suggested the presence of tetrameric RyR1 complexes composed of wild type and mutant subunits. The number of wild-type subunits to maintain a functional heterotetrameric channel differed among the four RyR1 mutants. The results indicate that homozygous RyR1 mutations associated with core myopathies abolish or greatly reduce sarcoplasmic reticulum Ca^{2+} release during excitation-contraction coupling. They further suggest that in individuals, expressing wild type and mutant alleles, a substantial portion of RyR1 channels is able to release Ca^{2+} from sarcoplasmic reticulum.

In skeletal muscle, an action potential causes voltage-dependent L-type Ca^{2+} channels localized in the cell membrane to activate closely apposed Ca^{2+} release channels known as ryanodine receptors (RyR1s)[2] (1). Massive release of Ca^{2+} from the sarcoplasmic reticulum (SR) into the myofibrillar space results in muscle contraction. Recent evidence indicates that impaired SR Ca^{2+} release is linked to RyR1 mutations and in affected individuals is associated with Central Core Disease (CCD) and Multiple Minicore Disease (MmD) (2–7). CCD is autosomal dominant disease, which results in the formation of large, centrally located cores or areas devoid of oxidizing enzymes and mitochondria. The majority of RyR1 mutations associated with CCD are located in the C-terminal, pore-forming region of RyR1. MmD is a recessive disease, characterized by the formation of multiple minicores. RyR1 MmD-related

[*]This work was supported by National Institutes of Health Grant AR018687. The costs of publication of this article were defrayed in part by the payment of page charges. This article must therefore be hereby marked "*advertisement*" in accordance with 18 U.S.C. Section 1734 solely to indicate this fact.

[S]The on-line version of this article (available at http://www.jbc.org) contains supplemental Figs. S1–S3.

[1]To whom correspondence should be addressed: Dept. of Biochemistry and Biophysics, University of North Carolina, Chapel Hill, NC 27599-7260. Tel.: 919-966-5021; Fax: 919-966-2852; meissner@med.unc.edu.

[2]The abbreviations used are: RyR, ryanodine receptor; RyR1, type 1 skeletal muscle RyR; E_{rev}, reversal potential; HEK, human embryonic kidney; P_O, channel open probability; SR, sarcoplasmic reticulum; RyR2, type 2 cardiac muscle RyR; RyR3, type 3 brain RyR; WT, wild type; CCD, Central Core Disease; MmD, Multiple Minicore Disease.

mutations appear to be distributed throughout the whole RyR1 genome and may result in silencing of one of the alleles in the affected individuals (6).

Ryanodine receptors (RyRs) are homotetrameric ion channels composed of four large 565-kDa subunits and four small 12-kDa subunits (8–10). RyRs have large conductances for both monovalent and divalent cations, while maintaining divalent *versus* monovalent selectivity. Fig. 1 shows a plausible model of the RyR1 ion pore (11). Two of the four subunits are removed for clarity. The model is based on the known structure of the K^+ channels (12) and shows a representation of the inner, most C-terminal, pore-forming, membrane-spanning segment, and a pore helix which is connected to an amino acid motif (GGGIG) that is similar to the selectivity filter motif (T(V/I)GYG) of K^+ channels. The model is in reasonable agreement with two cryoelectron microscopy studies that determined the pore structure of the closed channel at a resolution of ~10 Å (13,14). We identified by mutagenesis, in close proximity to the selectivity filter motif GGGIG, a conserved lumenal D4899/E4900 motif that has a critical role in RyR ion permeation and selectivity (15). Charge neutralization of two acidic residues (Asp-4938 and Asp-4945) in putative cytosolic vestibule reduced K^+ conductance, with D4938N also having a reduced Ca^{2+} selectivity (11). The results suggest that rings of lumenal and cytosolic negative charges determine ion fluxes by RyRs.

To better understand the pathophysiological function of RyR1 mutations associated with core myopathies, we investigated 3 CCD mutants in the C-terminal pore region (G4899E (3), G4899R (16), ΔV4927/I4928 (17)), and one MmD mutant (R109W/M485V (18)) in the N-terminal region of RyR1. Corresponding rabbit RyR1 mutants were expressed alone or together with wild type (WT) RyR1 in human embryonic kidney 293 (HEK 293) cells and single channel properties were determined following incorporation in lipid bilayers. The four mutants when expressed alone all showed variably decreased K^+ conductances and loss of Ca^{2+} conductance and Ca^{2+}-dependent gating. Co-expression of WT and mutant RyR1 subunits resulted in three groups of single channels that differed in their activity and ion permeability. Our results suggest that heterozygous expression of RyR1 core myopathy mutants may result in the assembly of (i) functional channels that are gated by Ca^{2+} and conduct Ca^{2+}, (ii) functional channels with a reduced Ca^{2+} conductance, and (iii) nonfunctional channels that do not conduct Ca^{2+}.

EXPERIMENTAL PROCEDURES

Materials

HEK 293 cells were obtained from ATCC and complete protease inhibitors from Roche Applied Science (Indianapolis, IN). Rabbit RyR1-G4898E and -G4898R mutants (corresponding to human CCD RyR1-G4899E and -G4899R) were kindly provided by Dr. Robert Dirksen (University of Rochester). Construction of rabbit RyR1-R110W and -R110W/L486V (18) (human RyR1-R109W and MmD RyR1-R109W/M485V, respectively), rabbit RyR1-D4899Q (15) and rabbit RyR1-ΔV4926/I4927 (19) (human CCD RyR1-ΔV4927/I4928) has been described. In this study, amino acid numbering is as described (20). Phospholipids were from Avanti Polar Lipids (Alabaster, AL). All chemicals were of analytical grade.

Expression of Wild Type and Mutant RyR1 Proteins in HEK 293 Cells

WT and mutant RyR1 cDNAs were transiently expressed in HEK 293 cells and transfected with FuGENE 6 (Roche Applied Science) according to the manufacturer's instructions. Cells were maintained at 37 °C and 5% CO_2 in high glucose Dulbecco's modified eagle medium containing 10% fetal bovine serum and plated the day before transfection. For each 10-cm tissue culture dish, 3.5 μg of cDNA was used. Cells were harvested 48 h after transfection. Crude membrane fractions (21) and proteoliposomes containing the purified WT and mutant RyR1 ion channels (22) were prepared in presence of protease inhibitors as described.

Immunoblot Analysis

Membrane fractions (20 μg of protein) representing the total particulate matter were separated by 3–12% SDS-PAGE, transferred to polyvinylidene difluoride membranes, and probed with polyclonal antibody for RyR1 (23). Western blots were developed using 3,3′-diaminobenzidine and H_2O_2 as substrates and quantified using UN-SCAN-IT (Silk Scientific Co) analysis software.

Stored Ca^{2+} Release

Stored Ca^{2+} release was determined using the fluorescent Ca^{2+} indicator dye Fluo 4-AM. HEK 293 cells were loaded with 5 μM Fluo 4-AM for 1 h at 37 °C in Krebs-Ringer-Henseleit (KRH) buffer (24). Individual cells were defined as regions of interest, and average fluorescence was measured by using ImageMaster program (Photon Technology International).

[^{3}H]Ryanodine Binding

Ryanodine binds with high specificity to the RyRs and is widely used to determine their protein expression levels (25). B_{max} values of [^{3}H]ryanodine binding were determined by incubating total particulate matter for 4 h at 24 °C with a saturating concentration of [^{3}H]ryanodine (30 nM) in 20 mM imidazole, pH 7.0, 0.6 M KCl, 0.15 M sucrose, protease inhibitors, and 100 μM Ca^{2+}. Specific [^{3}H]ryanodine binding was determined by a filtration assay as described (24).

Single Channel Recordings

Single channel measurements were performed using planar lipid bilayers containing a 5:3:2 mixture of bovine brain phosphatidylethanolamine, phosphatidylserine, and phosphatidylcholine (11). Proteoliposomes containing the purified recombinant RyR1s were added to the *cis* (SR cytosolic side) chamber of a bilayer apparatus and fused in the presence of an osmotic gradient (250 mM cis KCl/20 mM trans KCl in 20 mM KHepes, pH 7.4, 2 μM Ca^{2+}). After the appearance of channel activity, trans (SR lumenal) KCl concentration was increased to 250 mM. A strong dependence of single channel activities on cis Ca^{2+} concentration indicated that the large cytosolic “foot” region faced the cis chamber of the bilayers. The trans side of the bilayer was defined as ground. Electrical signals were filtered at 2 kHz (0.5 kHz for Ca^{2+} currents at 0 mV), digitized at 10 kHz, and analyzed as described (26).

To determine permeability ratios, single channel activities were recorded in symmetrical 250 mM KCl solution with 10 mM Ca^{2+} on the trans side and the reversal potential (E_{rev}) was measured. The permeability ratio of Ca^{2+} *versus* K^+ ions (P_{Ca}/P_K) was calculated using modified form of the Goldman-Hodgkin-Katz Equation 1,

$$E_{rev} = -\frac{RT}{F}\mathrm{Ln}\left\{[K]^{\frac{1}{2}} \times \left([K]+4\frac{P_{Ca}}{P_K}[\mathrm{Ca}]\right)^{-\frac{1}{2}}\right\} \quad \text{(Eq. 1)}$$

where [Ca] is the concentration of Ca^{2+} ions on trans side, and [K] is the concentration of K^+ ions on the cis and trans sides.

Biochemical Assays and Data Analysis

Free Ca^{2+} concentrations were obtained using solutions of Ca^{2+} and EGTA and were determined with a Ca^{2+}-selective electrode.

Results are given as mean ± S.E. Significance of differences in the data ($p < 0.05$) was determined using Student’s *t* test.

RESULTS

RyR1-D4899Q and RyR1 mutant channels associated with CCD and MmD were expressed alone or expressed together with WT-RyR1 in HEK293 cells to yield homotetrameric or heterotetrameric channel complexes. Fig. 1 shows the predicted location of RyR1-D4899Q (used as a control) and CCD-associated mutants RyR1-G4898E, -G4898R ("1"), and −ΔV4926/I4927 ("2"). The location of single site N-terminal RyR1-R110W and MmD-associated RyR1-R110W/L486V are not shown, as the two mutants are predicted to be a considerable distance away from the pore region of RyR1.

Expression Levels and Functional Properties of Mutant RyR1 Channels

Quantitative analysis of immunoblots showed that averaged protein levels of RyR1 mutants were within a factor of 2 of WT levels in HEK293 cells. HEK293 cells co-transfected with WT and mutant cDNAs in a 1:1 ratio had RyR1 protein bands with intensity comparable to WT (data not shown). The expression of functional RyR1 mutant channels was assessed by monitoring in HEK293 cells the fluorescence change in Fluo-4 in response to the addition of 10 mM caffeine and by determining B_{max} values of [^{3}H]ryanodine binding to membranes. With exception of G4898R, homotetrameric CCD and MmD mutants as well as RyR1-R110W showed a loss of function, as they failed to exhibit caffeine-induced Ca^{2+} release. Cells expressing G4898R showed reduced caffeine-induced Ca^{2+} release in 10–20% of cells compared with 50–60% in WT-expressing cells. All homotetrameric CCD and MmD mutants as well as RyR1-R110W bound negligible amounts of [^{3}H]ryanodine (not shown), which suggested that the mutations have a major impact on the structure of the channels leading to aberrant channel behavior. In agreement with a previous study (15), similar B_{max} values of [^{3}H]ryanodine binding were observed for cells expressing WT and D4899Q channels.

Single Channel Analysis of Homotetrameric RyR1 Channels

Detergent-solubilized WT and mutant channels were purified on sucrose gradients and reconstituted in proteoliposomes. WT and mutant channels migrated on the gradients as a single peak with an apparent sedimentation coefficient of ~30S, which indicated the presence of tetrameric channel complexes (27). Proteoliposomes containing the purified channel complexes were fused with planar lipid bilayers, and single channels were recorded in 250 mM KCl on both sides of the bilayer. The cis (cytosolic) bilayer chamber contained Ca^{2+} concentrations that either activated (2 μM) or only minimally activated (0.1 μM) WT-RyR1. In the *upper left trace* of Fig. 2*A*, a single partially activated WT-RyR1 channel is recorded in the presence of 2 μM free cytosolic Ca^{2+} at a bilayer potential of −35 mV. Reduction of cytosolic Ca^{2+} to 0.1 μM reduced channel open probability (P_o) to near zero (Fig. 2*A left, second trace*). Channel currents of mutant RyR1s with R110 W (Fig. 2*B*) and G4898E (Fig. 2*C*) or G4898R (Fig. 2*D*) substitution were reduced compared with WT. In contrast to WT, single channel open probabilities were not substantially reduced in presence of 0.1 μM cytosolic Ca^{2+} (Fig. 2, *B–D left, second traces*, Table 1). Control experiments with vector-transfected cells indicated that the above measurements were not performed with channel activities endogenously expressed in HEK 293 cells. Because RyR1-G4898R exhibited caffeine-induced Ca^{2+} release in HEK 293 cells, we also tested the ability of caffeine to activate the channel complex. We found that single RyR1-G4898R channel activities did not respond to 10 mM caffeine.

Currents through R110W, G4898E, and G4898R channels measured in symmetrical 250 mM KCl showed a linear voltage-dependence similar to WT-RyR1 (Fig. 2, *right*). Averaged conductances were 441 ± 75 pS for R110W, 410 ± 50 pS for G4898E, and 352 ± 61 pS for G4898R compared with 781 ± 7 pS for WT-RyR1 (Table 1).

To determine the ability of the mutant channels to conduct Ca^{2+}, WT and mutant channels were recorded in 250 mM symmetrical KCl with 10 mM Ca^{2+} in the trans (SR lumenal) bilayer chamber. WT exhibited averaged unitary Ca^{2+} current of −2.4 ± 0.1 pA at 0 mV (Fig. 2*A*, *left*, *third trace*, Table 1). Addition of 10 mM Ca^{2+} to the trans chamber reduced single channel currents at negative and positive potentials and yielded averaged reversal potential (E_{rev}) of +8.9 ± 0.1 mV (Fig. 2*A*, *right*, Table 1). Applying constant field theory by the equation given under "Experimental Procedures," an averaged permeability ratio of Ca^{2+} over K^+ (P_{Ca}/P_K) of 6.4 ± 0.1 was calculated (Table 1). In contrast, addition of 10 mM trans Ca^{2+} to the three mutant channels did not generate a noticeable unitary Ca^{2+} current at 0 m V and was without effect on currents or reversal potentials (Fig. 2, *B–D*, Table 1). Taken together, the single channel data indicate that the R110W and G4898E or G4898R substitutions introduced major alterations to the RyR1 channel pore. The three mutants showed negligible Ca^{2+} permeation, loss of Ca^{2+} responsiveness and exhibited a reduced conductance in symmetric KCl medium. The single channel properties of homotetrameric RyR1-R110W/L486V (18), RyR1-D4899Q (15) and RyR1-ΔV4926/I4927 (19) channels have been previously reported and are included in Table 1 for comparison.

Single Channel Analysis of Heterotetrameric RyR1 Channels

RyR1 is composed of four 565-kDa subunits. This suggests that simultaneous expression of mutant and WT-RyR1 subunits may result in the formation of heterotetrameric channel complexes and raises the question as to how these channels function in patients that carry both the WT and mutant alleles. We addressed this question by co-transfecting HEK 293 cells with WT and mutant cDNAs. Fig. 3*A* indicates the subunit distribution in channel complexes in cells expressing WT and mutants in 1:1 ratio, assuming a random distribution of the four subunits.

We initially performed experiments with heteromeric channel complexes composed of WT and D4899Q subunits, because these were expected to show marked differences in their K^+ conductance (Table 1). Single channels were recorded in 250 mM KCl on both sides of lipid bilayers. Weobserved in 38 single channel recordings five current levels (Fig. 3*B*). The averaged conductances were 795 ± 7 pS (n = 4), 632 ± 6 pS (n = 9), 483 ± 4 pS (n = 15), 300 ± 6 pS (n = 8), and 174 pS (n = 2). The highest and lowest currents levels were essentially identical to the averaged currents levels of homozygously expressed WT and D4899Q, respectively (Table 1). Single channel open probability did not vary significantly among the five groups of channel complexes (not shown). Multiple channel recordings were not analyzed. Reduction in cis Ca^{2+} from 2 μM to 0.1 μM Ca^{2+} reduced in all single channel recordings P_o close to zero, which indicated that the five receptor populations maintained Ca^{2+} sensitivity (not shown). In Fig. 3*E*, a plot of K^+ conductance *versus* group number yielded a straight line. To obtain the corresponding Ca^{2+} currents, channels were recorded at 0 mV in 250 mM symmetrical KCl in presence of 10 mM lumenal Ca^{2+} (Fig. 3*C*). Averaged unitary Ca^{2+} currents ranged from −2.4 ± 0.1 pA in Group 1 to −0.4 ± 0.1 pA in Group 5. Current-voltage relationships in presence of 10 mM lumenal Ca^{2+} yielded E_{rev} ranging from 8.9 ± 0.1 mV for Group 1 to 1.7 mV for Group 5 (Fig. 3*D*, Table 2). P_{Ca}/P_K ratios, calculated according to equation given under "Experimental Procedures," decreased with Group number parallel with K^+ conductance, except that channels in Groups 4 and 5 displayed a similar low permeability ratio close to 1 (Fig. 3*E*). Taken together, our findings suggest the presence of five groups of channel complexes having the six possible subunit distributions and arrangements shown in Fig. 3*A*. The results are best accounted for by the two channel configurations with two WT and two mutant subunits having a similar K^+ conductance and Ca^{2+} selectivity, and hence Groups 1, 2, 3, 4, and 5 having 0, 1, 2, 3, and 4 mutant subunits, respectively.

We next tested the possibility that WT and G4898E form heterotetrameric channel complexes with different ion permeation properties. HEK 293 cells were co-transfected with WT and mutant cDNAs at ratios ranging from 3:1 to 1:4. Fig. 4 shows a representative set of single channel recordings of co-expressed WT and G4898E channels in symmetric 250 m_M KCl in absence (*A*) and presence (*B*) of 10 m_M lumenal Ca^{2+}. According to reversal potentials in presence of 10 m_M lumenal Ca^{2+} (Fig. 4*C*, Table 2), five groups of single channels were observed. Twenty-six channels (Groups 1–4 in Fig. 4, *A* and *D*) maintained Ca^{2+}-dependent channel activity and had a K^+ conductance comparable to WT. Of these, 11 single channels had P_{Ca}/P_K comparable to WT, which suggested that homotetrameric WT channels were recorded. The remaining 15 channels had lower P_{Ca}/P_K values of 5.1 ± 0.1 (n = 8), 4.1 ± 0.2 (n = 5) and 2.6 ± 0.2 (n = 2), which suggested the presence of three groups (Groups 2–4 in Fig. 4*D*) of functional hybrid channels composed of WT and G4898E subunits. Single channel open probability at 2 μ_M cis Ca^{2+} did not significantly differ among Groups 1–4. Ten channels (Group 5 in Fig. 4) showed a channel behavior similar to homozygously expressed mutant channels. K^+ conductance was reduced and Ca^{2+} dependent activity and Ca^{2+} permeation were not observed. Taken together, data of Fig. 4 and Table 2 indicate the presence of homotetrameric WT and G4898E channels and 3 different groups of WT:G4898E hybrid channels. The results with the hybrid channels are best rationalized by the channel complexes of Groups 2–4 having 1, 2, and 3 mutant subunits, respectively.

As with D4899Q and G4898E, multiple groups of channels could be distinguished when HEK 293 cells were co-transfected with WT and G4898R, R110W, R110W/L486V, or ΔV4926/I4927 RyR1 cDNAs in ratios ranging from 3:1 to 1:4 (Fig. 5 and supplemental Figs. S1–S3). The ion permeation properties of purified channel complexes were determined in symmetric 250 m_M KCl in absence and presence of 10 m_M lumenal Ca^{2+} as described above. The results of these studies are summarized in Fig. 5, *A–C*. *Solid* and *open symbols* show channels that maintained Ca^{2+} sensitivity. Symbols with x-hair represent channels that did not respond to a change in Ca^{2+} concentration. Unexpectedly, channel complexes composed of WT and G4898E or G4898R subunits exhibited essentially identical ion permeation properties (Fig. 5*A*). Substitution of glycine residue with a negative or positive charge in the selectivity filter of RyR1 yielded three groups of hybrid channels that exhibited the same reversal potentials (Table 2) and intermediate Ca^{2+} over K^+ permeability ratios (Fig. 5*A*). In both cases, channels with 1, 2, or 3 predicted mutant subunits (Groups 2–4) maintained Ca^{2+} sensitivity and exhibited K^+ conductances comparable to WT. Fig. 5*B* and Table 2 show that, according to the reversal potentials, only four groups of single channels could be detected when WT-RyR1 and RyR1-ΔV4926/I4927 were co-expressed in HEK293 cells. In 20 single channel recordings, 14 channels (Groups 1–3) maintained Ca^{2+}-dependent channel activity and had a K^+ conductance comparable to WT. Of these, 5 channels had P_{Ca}/P_K ratio comparable to WT, which suggested that homotetrameric WT channels were recorded. The remaining 9 channels had lower P_{Ca}/P_K values of 5.4 ± 0.1 (n = 6) and 3.9 ± 0.2 (n = 3). We suggest that hybrid channels with one and two mutant subunits, respectively, were recorded, as it is unlikely that channels with 3 but not 1 mutant subunit maintained Ca^{2+}-dependent channel activity. Six channels (Group 5 in Fig. 5*B*) showed a channel behavior similar to homozygously expressed mutant channels. K^+ conductance was reduced and no Ca^{2+}-dependent activity or Ca^{2+} permeation were observed.

Homotetrameric N-terminal MmD-related RyR1-R110W/L486V exhibited an aberrant single channel behavior comparable to C-terminal, CCD-associated RyR1 mutants (Table 1). To better understand the underlying mechanisms leading to loss of Ca^{2+} responsiveness and Ca^{2+} permeation, we tested the ability of R110W/L486V mutant to form functional heteromeric channels with WT-RyR1. Because Leu-486 in the rabbit sequence is not conserved in two affected individuals, who carried the corresponding M485V mutation in addition to R109W (18), we also examined single channel properties of WT:R110W hybrid channels. Co-

expression of WT and R110W resulted in channel complexes with reversal potentials and P_{Ca}/P_K ratios ranging from those for homotetrameric WT to homotetrameric mutant channels (P_{Ca}/P_K = 6.4 and 0, 7 and 4 of 30 recordings, respectively) (Fig. 5*C*). Channel complexes with intermediate P_{Ca}/P_K ratios of 5.1 ± 0.1 (n = 13), 3.9 ± 0.2 (n = 3), and 2.9 ± 0.1 (n = 3) maintained Ca^{2+} responsiveness and exhibited K^+ conductances comparable to WT. By comparison, co-expression of WT and R110W/L486V resulted in formation of channel complexes that predominantly exhibited a single channel behavior either comparable to WT-RyR1 (7 of 25 recordings) or RyR1-R110W/L486V (13 of 25 recordings) (Fig. 5*C*). In the remaining 5 recordings, channels maintained Ca^{2+} sensitivity and had K^+ conductance comparable to WT. Single channel measurements yielded only one intermediate P_{Ca}/P_K value of 5.7. The results suggest that hybrid channels composed of WT and R110W subunits, and to a smaller extent composed of WT and R110W/L486V subunits, form functional channels that conduct Ca^{2+} and respond to a change in cytosolic Ca^{2+}.

DISCUSSION

The ryanodine receptor has a key role in skeletal muscle excitation-contraction coupling by releasing Ca^{2+} required for muscle contraction. Ample evidence has been recently provided that RyR1 mutations associated with core myopathies exhibit an impaired SR Ca^{2+} release. The functional properties of RyR1 core myopathy mutants composed of both WT and mutant subunits, however, have remained unclear. Herein, we describe single channel measurements that enabled us to gain novel insights on the function of heterozygously expressed CCD and MmD mutants of RyR1. We examined the functional properties of these mutations on RyR1 function, following their expression in HEK 293 cells, purification and incorporation in lipid bilayers. Initial experiments revealed that three homozygously expressed CCD mutants in the C-terminal pore region of RyR1 and one N-terminal MmD mutant all showed negligible Ca^{2+} permeation and loss of Ca^{2+}-dependent gating but maintenance of reduced K^+ conductance. Subsequent co-expression of WT and mutant RyR1s resulted in three distinct types of single channels (see Scheme 1). Channels had activities comparable to homozygously expressed WT or mutant channels. A third group of channels maintained Ca^{2+}-dependent activity and K^+ conductance comparable to WT but exhibited Ca^{2+} selectivities compared with K^+ intermediate between WT and mutant channels. Our results further suggest that the number of WT subunits to maintain a functional channel differed among the four RyR1 mutants examined in the present study (Scheme 1).

The most straightforward test of forming heterotetrameric channels involved RyR1-D4899Q. Replacement of aspartate residues immediately following the GGGIG motif with glutamine residues greatly reduces ion permeation and selectivity, without loss of regulation by Ca^{2+} (15). It is therefore unlikely that the mutation has a major impact on the global structure of the channel. The distribution of homotetrameric and heterotetrameric channel complexes did not strictly depend on transfection ratio of WT to mutant cDNAs and could not be directly determined; however, six different arrangements of WT and mutant subunits are possible (Fig. 3*A*). Accordingly, four types of heterotetrameric channel complexes may be formed, each having distinct ion permeation properties. Indeed, co-expression of cardiac muscle WT-RyR2 (28) or brain RyR (RyR3) (29) with RyR2-G4824A (analogous to G4894A in RyR1) produced four intermediate K^+ conductances. We detected only three well-defined, intermediate K^+ conductances. This suggests that the decrease in ion permeation and selectivity was a direct result of the charge being reduced by the D4899Q mutation, and hence was largely independent of the two possible arrangements of the two WT and two mutant subunits (Fig. 3*A*).

In contrast to the experimental D4899Q mutant, K^+ conductances were maintained in heteromeric CCD and MmD mutants that responded to a change in cytosolic Ca^{2+} concentration (Fig. 5). K^+ conductances comparable to WT were maintained in channel

complexes containing three predicted (R110W/L486V), two (ΔV4926/I4927), or only one (G4898E, G4898R) wild type subunit. The results suggest that a pore structure close to WT was maintained. In support of this suggestion, only mutant channel complexes that responded to a change in Ca^{2+} maintained a K^+-conductance comparable to WT. We also note that the four 4899 aspartate residues were maintained in the heteromeric mutant channels, as compared with heteromeric RyR1-D4899Q mutant channels. On the other hand, the P_{Ca}/P_K ratio varied among heteromeric channel complexes that responded to a change in Ca^{2+} (Fig. 5). We conclude that the CCD and MmD subunits induced in these channels structural changes that attenuated the ability of divalent Ca^{2+} cations to pass through the pore while having little consequences on monovalent K^+ conductances.

RyR1-G4898E and -G4898R mutations substitute a well conserved amino acid residue of the RyR GGGIGDE motif (Fig. 1). The two mutations were linked to CCD in several unrelated families (3,16,30). Homozygous expression of CCD mutations RyR1-G4898E and −G4898R in myotubes lacking RyR1 resulted in minimal caffeine-induced Ca^{2+} release, which suggested that the two mutants did not release significant amounts of Ca^{2+} from SR (31). On the other hand, immortalized lymphoblasts (16) and HEK cells (32) carrying WT and G4898E alleles released reduced amounts of Ca^{2+} in response to 4-chloro-m-cresol and caffeine, two activators of RyR1, which suggested the presence of functional but leaky RyR ion channels. The present study reveals that homozygous expression of G4898E resulted in loss of caffeine-induced Ca^{2+} release and in the case of G4898R in unstable channel complexes. HEK 293 cells expressing G4898R showed a reduced Ca^{2+} release in response to caffeine. Negligible [^{3}H] ryanodine binding to G4898R indicated loss of function during membrane isolation. In single channel measurements, G4898R and G4898E showed loss of regulation by Ca^{2+} and negligible Ca^{2+} permeation but maintenance of reduced K^+ conductance. Co-expression with WT in HEK293 cells yielded five groups of channel complexes with ion permeation and selectivity properties essentially identical for the two mutations, despite the replacement of glycine with a negatively or positively charged residue. This suggests that the negatively and positively charged side chains are held in a configuration that avoided a direct interaction with the conducting ions. Rescue of WT K^+ conductance and Ca^{2+} regulation by only one WT subunit suggests that the conformational alterations induced by the mutations involve relatively weak interactions with other residues. On the other hand, an only partial restoration of Ca^{2+} over K^+ selectivity suggests that one mutant subunit was sufficient to alter the pore structure. A more detailed understanding of the conformational changes associated with the two mutations will require that the solution structure of the RyR pore region becomes available.

CCD-linked RyR1-ΔV4926/I4927 deletions are located in the predicted inner, most C-terminal, membrane-spanning segment of the channel (Fig. 1). The deletion was identified as a novel mutation in one patient (17). Wang *et al.* (33,34) mutated the residues within the membrane-spanning segment of the cardiac ryanodine receptor (RyR2) to alanine and found that RyR2-V4854A and -I4855A (matching RyR1-V4926 and -I4927 deletion sites) retained function but showed a reduced response to caffeine activation. We previously showed that deletion of RyR1 residues Val-4926 and Ile-4927 results in a nonfunctional channel unable to conduct Ca^{2+} (19). The present study shows that co-expression of WT and RyR1-ΔV4926/I4927 resulted in formation of two groups of functional channels that showed a reduced Ca^{2+} over K^+ permeability ratio. Both groups responded to a change in cytosolic Ca^{2+} and maintained a normal K^+ conductance. The results suggest that the presence of two WT subunits is required to form functional heteromeric WT:ΔV4926/I4927 channel complexes, as compared with only one WT subunit in WT:G4898E and WT:G4898R channel complexes. However, we cannot rule out that WT:ΔV4926/I4927 channels with one WT subunit are structurally unstable outside of the intact cellular environment and were therefore not observed in single channel measurements.

The effects of MmD RyR1-R110W/L486V mutation in N-terminal region are complex. In two affected siblings who carried the corresponding R109W and M485V mutations, only the mutated allele was transcribed in skeletal muscle, as determined by RT-PCR (18). Homozygous expression of recombinant RyR1-R110W and RyR1-R110W/L486V resulted in loss of Ca^{2+} sensitivity and Ca^{2+} permeation and similarly reduced K^+ conductance (Table 1). Co-expression studies indicated that RyR1-R110W had a higher propensity to form functional channels with WT than RyR1-R110W/L486V. R110W formed three groups of heteromeric channels in contrast to R110W/L486V, which showed only one group of channels with a reduced Ca^{2+} over K^+ selectivity compared with WT. Hence, both R110W and L486V cause conformational changes involved in loss of channel function. Second, there appears to exist a strong interaction between N-terminal and C-terminal regions of RyR1 affecting Ca^{2+} conductance and Ca^{2+}-dependent gating.

We have previously presented a Poisson Nernst Plank-Density Functional Theory (PNP-DFT) model that suggests charge-space competition determines the ion permeation and selectivity properties of RyR1 (35). The model predicts that negatively charged Asp-4899 forms part of the selectivity filter and due to the high concentration of its negatively charged oxygen atoms dominates the ion permeation and selectivity properties of WT-RyR1. High K^+ conductance arises because of a high K^+ concentration in the selectivity filter, and selectivity because the more highly charged and smaller Ca^{2+} is able to replace K^+ in the pore. The model predicts that replacement of Asp-4899 with glutamine or asparagine residues reduces K^+ conductance and Ca^{2+} selectivity compared with K^+. The results of the present study suggest that the decrease in ion permeation and selectivity is nearly proportional to the charge being reduced by the D4899Q mutation (Fig. 3). In contrast to the experimental D4899Q mutant, K^+ conductance was maintained in channel complexes that responded to a change in cytosolic Ca^{2+} concentration and contained one to three CCD and MmD mutants (Fig. 5). In comparison, Ca^{2+} selectivity compared with K^+ showed a relationship close to D4899Q, *i.e.* the P_{Ca}/P_K ratio depended on the predicted number of mutant subunits (Fig. 5). We propose that the CCD and MmD subunits induce structural changes that attenuate the ability of Ca^{2+} to compete with K^+.

Core myopathies exhibit a great variability both clinically and histologically (2–7). The severity of the symptoms may even vary within the same family. This has suggested that many factors need to be considered. Recent studies suggest that recessive MmD mutations may alter the proportion of functional RyR1 channels by suppressing expression of the WT allele (18, 36). Zebrafish relatively relaxed mutants have reduced ryanodine receptor protein levels that are associated with amorphous cores and are developmentally regulated due to aberrant splicing of RyR mRNA (37). RyR1 is regulated by associated proteins (8,10) that may alter mutant channel structure and function in skeletal muscle and contribute to pathological variability of core myopathies. The data of the present study reveal an additional mechanism. Our single channel analysis demonstrates that co-expression of WT-RyR1 with RyR1 mutants associated with core myopathies results in the formation of homotetrameric and heterotetrameric channels. Homotetrameric mutant channels conducted negligible amounts of Ca^{2+} and were not regulated by Ca^{2+}. The number of WT subunits in heteromeric channels required to restore Ca^{2+} regulation and Ca^{2+} permeation depended on the mutation. Our results suggest that the fraction of functional channels in patients carrying both the WT and mutant allele varies among the different missense and deletion mutations associated with CCD and MmD, and hence may provide one mechanism that determines the phenotypic diversity of core myopathies.

Supplementary Material

Refer to Web version on PubMed Central for supplementary material.

REFERENCES

1. Rios E, Pizarro G. Physiol. Rev 1991;71:849–908. [PubMed: 2057528]
2. McCarthy TV, Quane KA, Lynch PJ. Hum. Mutat 2000;15:410–417. [PubMed: 10790202]
3. Monnier N, Romero NB, Lerale J, Landrieu P, Nivoche Y, Fardeau M, Lunardi J. Hum. Mol. Genet 2001;10:2581–2592. [PubMed: 11709545]
4. Dirksen RT, Avila G. Trends Cardiovasc. Med 2002;12:189–197. [PubMed: 12161072]
5. Zorzato F, Jungbluth H, Zhou H, Muntoni F, Treves S. IUBMB Life 2007;59:14–20. [PubMed: 17365175]
6. Zhou H, Jungbluth H, Sewry CA, Feng L, Bertini E, Bushby K, Straub V, Roper H, Rose MR, Brockington M, Kinali M, Manzur A, Robb S, Appleton R, Messina S, D'Amico A, Quinlivan R, Swash M, Muller CR, Brown S, Treves S, Muntoni F. Brain 2007;130:2024–2036. [PubMed: 17483490]
7. Robinson R, Carpenter D, Shaw MA, Halsall J, Hopkins P. Hum. Mutat 2006;27:977–989. [PubMed: 16917943]
8. Fill M, Copello JA. Physiol. Rev 2002;82:893–922. [PubMed: 12270947]
9. Franzini-Armstrong C, Protasi F. Physiol. Rev 1997;77:699–729. [PubMed: 9234963]
10. Meissner G. Front. Biosci 2002;7:d2072–d2080. [PubMed: 12438018]
11. Xu L, Wang Y, Gillespie D, Meissner G. Biophys. J 2006;90:443–453. [PubMed: 16239337]
12. Jiang Y, Lee A, Chen J, Cadene M, Chait BT, MacKinnon R. Nature 2002;417:523–526. [PubMed: 12037560]
13. Samso M, Wagenknecht T, Allen PD. Nat. Struct. Mol. Biol 2005;12:539–544. [PubMed: 15908964]
14. Ludtke SJ, Serysheva II, Hamilton SL, Chiu W. Structure 2005;13:1203–1211. [PubMed: 16084392]
15. Wang Y, Xu L, Pasek DA, Gillespie D, Meissner G. Biophys. J 2005;89:256–265. [PubMed: 15863483]
16. Tilgen N, Zorzato F, Halliger-Keller B, Muntoni F, Sewry C, Palmucci LM, Schneider C, Hauser E, Lehmann-Horn F, Muller CR, Treves S. Hum. Mol. Genet 2001;10:2879–2887. [PubMed: 11741831]
17. Davis MR, Haan E, Jungbluth H, Sewry C, North K, Muntoni F, Kuntzer T, Lamont P, Bankier A, Tomlinson P, Sanchez A, Walsh P, Nagarajan L, Oley C, Colley A, Gedeon A, Quinlivan R, Dixon J, James D, Muller CR, Laing NG. Neuromuscul. Disord 2003;13:151–157. [PubMed: 12565913]
18. Zhou H, Yamaguchi N, Xu L, Wang Y, Sewry C, Jungbluth H, Zorzato F, Bertini E, Muntoni F, Meissner G, Treves S. Hum. Mol. Genet 2006;15:2791–2803. [PubMed: 16940308]
19. Lyfenko AD, Ducreux S, Wang Y, Xu L, Zorzato F, Ferreiro A, Meissner G, Treves S, Dirksen RT. Hum. Mutat 2007;28:61–68. [PubMed: 16958053]
20. Takeshima H, Nishimura S, Matsumoto T, Ishida H, Kangawa K, Minamino N, Matsuo H, Ueda M, Hanaoka M, Hirose T, Numa S. Nature 1989;339:439–445. [PubMed: 2725677]
21. Gao L, Balshaw D, Xu L, Tripathy A, Xin C, Meissner G. Biophys. J 2000;79:828–840. [PubMed: 10920015]
22. Lee HB, Xu L, Meissner G. J. Biol. Chem 1994;269:13305–13312. [PubMed: 8175760]
23. Du W, McMahon TJ, Zhang ZS, Stiber JA, Meissner G, Eu JP. J. Biol. Chem 2006;281:30143–30151. [PubMed: 16891657]
24. Wang Y, Xu L, Duan H, Pasek DA, Eu JP, Meissner G. J. Biol. Chem 2006;281:15572–15581. [PubMed: 16595676]
25. Sutko JL, Airey JA, Welch W, Ruest L. Pharmacol. Rev 1997;49:53–98. [PubMed: 9085309]
26. Xu L, Tripathy A, Pasek DA, Meissner G. J. Biol. Chem 1999;274:32680–32691. [PubMed: 10551824]
27. Lai FA, Misra M, Xu L, Smith HA, Meissner G. J. Biol. Chem 1989;264:16776–16785. [PubMed: 2550460]
28. Zhao M, Li P, Li X, Zhang L, Winkfein RJ, Chen SR. J. Biol. Chem 1999;274:25971–25974. [PubMed: 10473538]
29. Xiao B, Masumiya H, Jiang D, Wang R, Sei Y, Zhang L, Murayama T, Ogawa Y, Lai FA, Wagenknecht T, Chen SR. J. Biol. Chem 2002;277:41778–41785. [PubMed: 12213830]

30. Romero NB, Monnier N, Viollet L, Cortey A, Chevallay M, Leroy JP, Lunardi J, Fardeau M. Brain 2003;126:2341–2449. [PubMed: 12937085]

31. Avila G, O'Connell KM, Dirksen RT. J. Gen. Physiol 2003;121:277–286. [PubMed: 12642598]

32. Du GG, Khanna VK, Guo X, MacLennan DH. Biochem. J 2004;382:557–564. [PubMed: 15175001]

33. Wang R, Bolstad J, Kong H, Zhang L, Brown C, Chen SR. J. Biol. Chem 2004;279:3635–3642. [PubMed: 14593104]

34. Wang R, Zhang L, Bolstad J, Diao N, Brown C, Ruest L, Welch W, Williams AJ, Chen SR. J. Biol. Chem 2003;278:51557–51565. [PubMed: 14557272]

35. Gillespie D, Xu L, Wang Y, Meissner G. J. Phys. Chem. B 2005;109:15598–155610. [PubMed: 16852978]

36. Zhou H, Brockington M, Jungbluth H, Monk D, Stanier P, Sewry CA, Moore GE, Muntoni F. Am. J. Hum. Genet 2006;79:859–868. [PubMed: 17033962]

37. Hirata H, Watanabe T, Hatakeyama J, Sprague SM, Saint-Amant L, Nagashima A, Cui WW, Zhou W, Kuwada JY. Development 2007;134:2771–2781. [PubMed: 17596281]

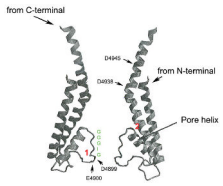

FIGURE 1. Hypothetical model for ion pore of RyR1

The RyR1 pore model (taken from Ref. 11) shows the GGGIG motif (residues 4894–4898) and positions of lumenal amino acid residues Asp-4899 and Glu-4900, cytosolic residues Asp-4938 and Asp-4945, and CCD residues Gly-4898 (“1”) and Val-4926/Ile-4927 (“2”). Note only two of the four pore-forming segments are shown.

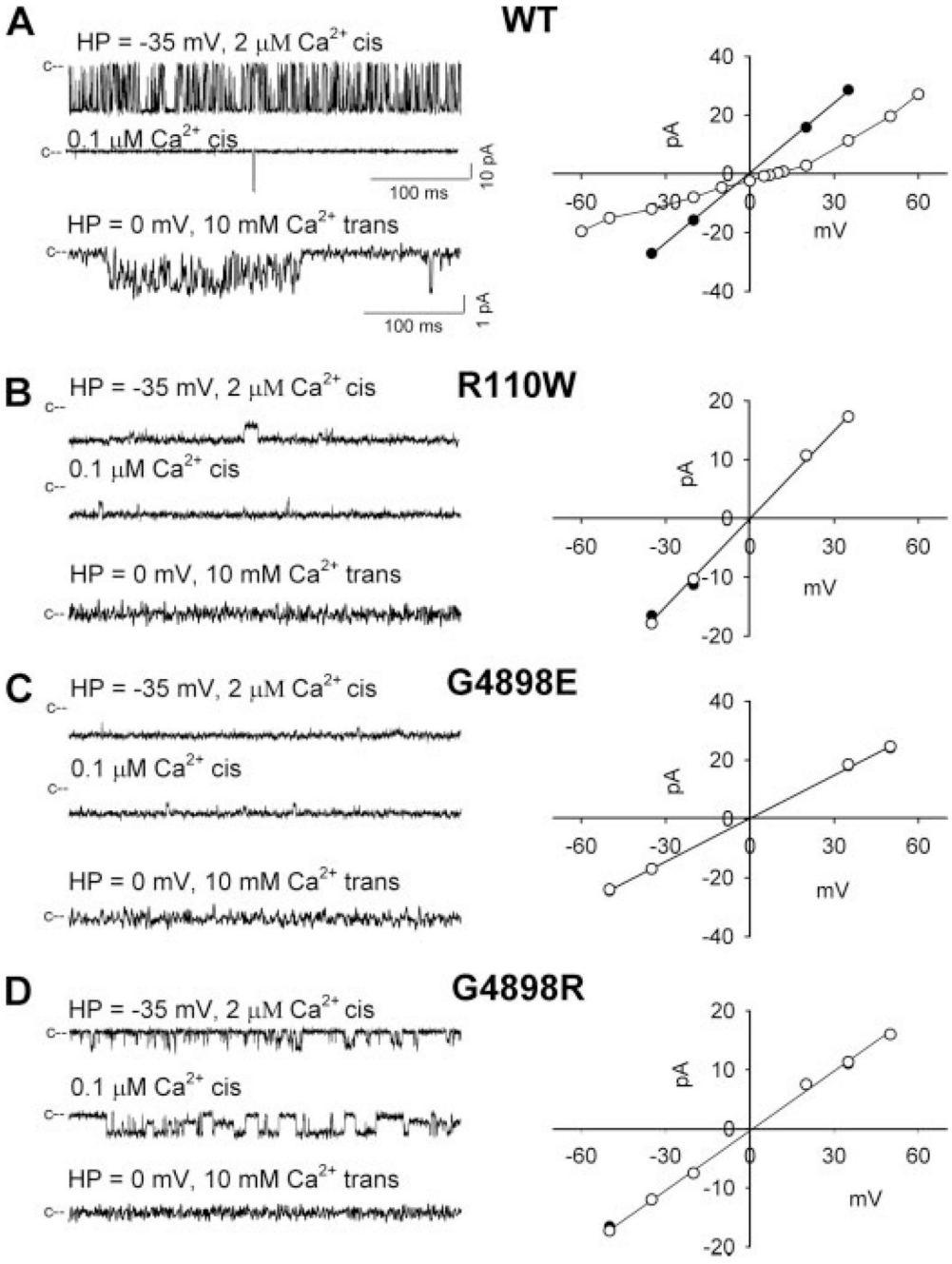

FIGURE 2. Single channel recordings of homotetrameric WT and mutant RyR1 channels

A, single channel currents were recorded at −35 mV (*upper* and *middle traces*) or 0 mV (*bottom traces*) as downward inflections from the closed state (c−) in symmetrical 250 mM KCl with 2 μM Ca^{2+} in the cis chamber (*upper traces*) and following the subsequent addition of EGTA to yield free cis Ca^{2+} concentration of 0.1 μM (*second trace*) or the addition of 10 mM trans Ca^{2+} (*third trace*) (*left panels*). Representative current voltage relationships in 250 mM symmetrical KCl (●) and after the subsequent addition of 10 mM trans Ca^{2+} (○) (*right panels*). In *B–D*, overlap of data hides *solid circles*. Averaged currents and reversal potentials (E_{rev}) are summarized in Table 1.

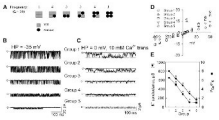

FIGURE 3. Single channel recordings of homotetrameric and heterotetrameric WT and D4899Q channel complexes

A, subunit distribution and frequency of channel complexes in cells expressing WT and mutant subunits at 1:1 ratio, assuming a random distribution of subunits. *B*, single channel currents were recorded at −35 mV in symmetrical 250 mM KCl with 2 μM cis Ca^{2+} as downward inflections from the closed state (c−). *C*, single channel currents after addition of 10 mM trans Ca^{2+} at 0 mV as downward inflections from the closed state (c−) to open states (*dashed line*). *D*, representative current voltage relationships in 250 mM symmetrical KCl in presence of 10 mM trans Ca^{2+}. *E*, K^+ conductances and permeability ratios of 5 groups of channels. *, $p < 0.05$ compared with the preceding group.

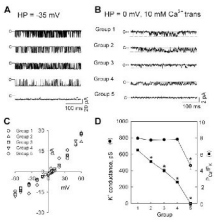

FIGURE 4. Single channel recordings of homotetrameric and heterotetrameric WT and G4898E channel complexes

A, single channel currents were recorded at −35 mV in symmetrical 250 mM KCl with 2 μM cis Ca^{2+} as downward inflections from the closed state (c−). *B*, after addition of 10 mM trans Ca^{2+} at 0 mV as downward inflections from the closed state (c−) to open states (*dashed line*). *C*, representative current voltage relationships in 250 mM symmetrical KCl in presence of 10 mM trans Ca^{2+}.*D*, K^+ conductances and permeability ratios of 5 groups of channels. Symbols with cross-hair (Group 5) indicate data for mutant channels that did not respond to a change in cytosolic Ca^{2+}. *, $p < 0.05$ compared with the preceding group.

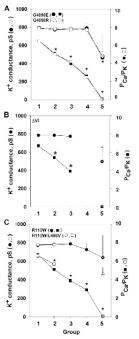

FIGURE 5. K^+ conductances and permeability ratios of homotetrameric and heterotetrameric WT and mutant channels

Symbols with cross-hair (Group 5) indicate data for mutant channels that did not respond to a change in cytosolic Ca^{2+}.

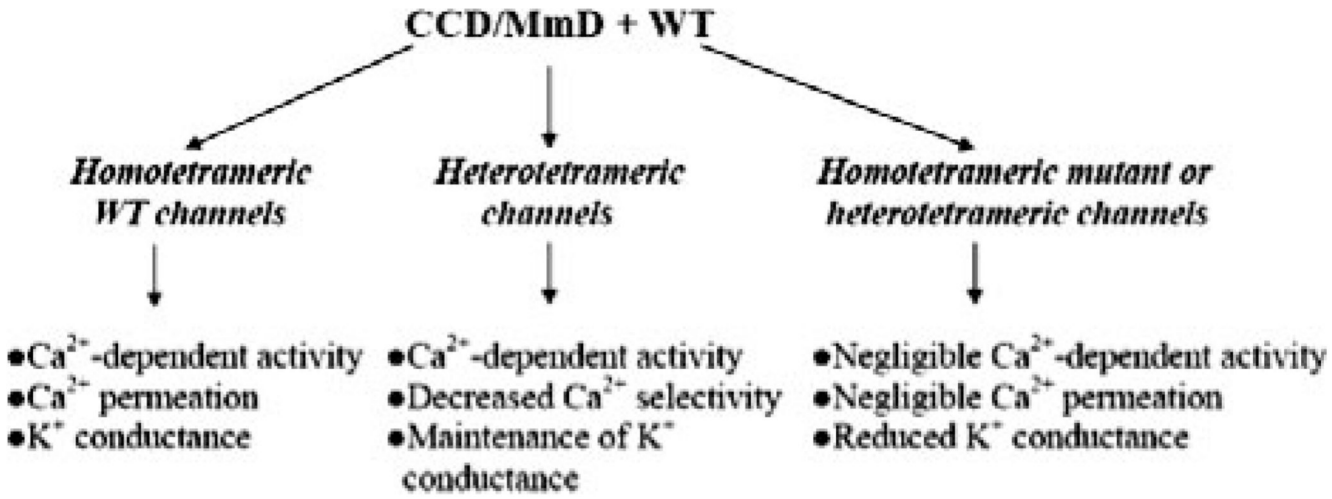

SCHEME 1.

TABLE 1

Single channel properties of homotetrameric WT and mutants in symmetric KCl solution

	P_o		γ	I_o	E_{rev}	P_{Ca}/P_K
	2 μM cis Ca^{2+}	**0.1 μM cis Ca^{2+}**		**10 mM trans Ca^{2+}**		
			pS	*pA*	*mV*	
WT-RyR1	0.27 ± 0.08 (9)[a]	0.004 ± 0.003 (7)	781 ± 7 (12)	−2.4 ± 0.1 (12)	8.9 ± 0.1 (12)	6.4 ± 0.1 (12)
R110W	0.61 ± 0.18 (6)	0.50 ± 0.20 (3)	441 ± 75 (8)	≤0.1 (4)	<0.3 (5)	ND[b]
R110W/L486V	0.64 ± 0.15 (7)	0.60 ± 0.23 (3)	442 ± 77 (9)	≤0.1 (4)	<0.3 (4)	ND
G4898E	0.41 ± 0.16 (9)	0.56 ± 0.16 (7)	410 ± 50 (11)	≤0.1 (7)	<0.3 (7)	ND
G4898R	0.34 ± 0.12 (9)	0.25 ± 0.13 (6)	352 ± 61 (10)	≤0.1 (6)	<0.3 (6)	ND
D4899Q	0.33 ± 0.10 (9)	0.0002 ± 0.0001 (8)	164 ± 4 (10)	−0.4 ± 0.1 (4)	1.7 ± 0.2 (4)	1.0 ± 0.2 (4)
ΔV4926/I4927	0.67 ± 0.13 (10)	0.92 ± 0.02 (3)	621 ± 66 (14)	≤0.1 (5)	<0.3 (5)	ND

[a] Number in parentheses indicates number of determinations.

[b] ND, not determined.

J Biol Chem. Author manuscript; available in PMC 2010 October 18.

TABLE 2

Reversal potentials of homotetrameric and heterotetrameric WT and mutant channel complexes in symmetric KCl solution in the presence of 10 m_M lumenal Ca^{2+}

	E_{rev}				
	Group 1	**Group 2**	**Group 3**	**Group 4**	**Group 5**
	mV	*mV*	*mV*	*mV*	*mV*
R110W	9.1 ± 0.2 (7)[a]	7.5 ± 0.1 (13)[b]	6.1 ± 0.2 (3)[b]	4.8 ± 0.1 (3)[b]	<0.3 (4)[b]
R110W/L486V	9.1 ± 0.2 (7)	8.1 ± 0.1 (5)[b]	ND[c]	ND	<0.3 (13)
G4898E	8.9 ± 0.1 (11)	7.5 ± 0.1 (8)[b]	6.2 ± 0.2 (5)[b]	4.4 (2)	<0.3 (10)[b]
G4898R	9.0 ± 0.2 (5)	7.4 ± 0.1 (7)[b]	6.4 ± 0.1 (6)[b]	4.5 ± 0.4 (4)[b]	<0.3 (6)[b]
D4899Q	8.9 ± 0.1 (4)	7.3 ± 0.3 (4)[b]	4.9 ± 0.2 (4)[b]	1.9 ± 0.6 (3)[b]	1.7 (2)
ΔV4926/I4927	9.0 ± 0.2 (5)	7.8 ± 0.1 (6)[b]	6.1 ± 0.3 (3)[b]	ND	<0.3 (6)

[a] Number in parentheses indicates number of determinations.

[b] $p < 0.05$ compared to preceding group.

[c] ND, not determined.

J Biol Chem. Author manuscript; available in PMC 2010 October 18.